

Cluster Compounds Bearing both High- and Low-Valent Transition Metal Fragments: The Reactions of Imido Carbonyl Cluster $\text{Ru}_3(\text{CO})_{10}(\mu_3\text{-NPh})$ with Dioxo Acetylide Complexes $(\text{C}_5\text{Me}_5)\text{W}(\text{O})_2(\text{CCR})$, $\text{R} = \text{Ph}$ and $\text{CMe}=\text{CH}_2$

Chih-Wei Pin,[†] Yun Chi,^{*,†} Cathy Chung,[†] Arthur J. Carty,^{*,‡} Shie-Ming Peng,[§] and Gene-Hsing Lee[§]

Department of Chemistry, National Tsing Hua University, Hsinchu 30043, Taiwan, Republic of China, Steacie Institute for Molecular Sciences, National Research Council Canada, 100 Sussex Drive, Ottawa, Ontario, Canada K1A 0R6, and Department of Chemistry and Instrumentation Center, National Taiwan University, Taipei 10764, Taiwan, Republic of China

Received April 21, 1998

Heterobimetallic compounds $(\text{C}_5\text{Me}_5)\text{W}(\text{O})(\mu\text{-O})\text{Ru}_3(\mu_3\text{-NPh})(\text{CCR})(\text{CO})_8$, $\text{R} = \text{Ph}$ and $\text{CMe}=\text{CH}_2$ (**1a** and **1b**), which contain the high oxidation state dioxo tungsten fragment and the low-valent ruthenium carbonyl unit, were obtained from the reaction of $\text{Ru}_3(\mu_3\text{-NPh})(\text{CO})_{10}$ with $(\text{C}_5\text{Me}_5)\text{W}(\text{O})_2(\text{CCR})$, $\text{R} = \text{Ph}$ and $\text{CMe}=\text{CH}_2$. These complexes consist of an open triangular Ru_3 core with the dioxo tungsten unit coordinated to the central Ru atom via a $\text{W}=\text{O} \rightarrow \text{Ru}$ dative interaction. Conversion to the pentametallic complex $(\text{C}_5\text{Me}_5)\text{W}(\text{O})(\mu\text{-O})\text{Ru}_4(\mu_3\text{-PPh})(\text{CCPh})(\text{CO})_{10}$ (**2**) was realized by treatment of **1a** with $\text{Ru}_3(\text{CO})_{12}$ in refluxing toluene, while heating a solution of **1b** led to the isolation of $(\text{C}_5\text{Me}_5)\text{W}(\mu\text{-O})_2\text{Ru}_3(\mu_3\text{-NPh})(\text{CCMe}=\text{CH}_2)(\text{CO})_6$ (**4**) through the removal of two CO ligands. Reaction of **4** with PMe_2Ph was examined, giving the monosubstituted $(\text{C}_5\text{Me}_5)\text{W}(\mu\text{-O})_2\text{Ru}_3(\text{CCMe}=\text{CH}_2)(\mu_3\text{-NPh})(\text{CO})_5(\text{PMe}_2\text{Ph})$ (**5**) in moderate yield, of which the X-ray diffraction study lends support to the identification of its precursor **4**. The reactivity of complex **4** with CO was then established, affording $(\text{C}_5\text{Me}_5)\text{W}(\mu\text{-O})_2\text{Ru}_3(\mu_3\text{-NPh})(\text{CCMe}=\text{CH}_2)(\text{CO})_7$ (**6**) and $(\text{C}_5\text{Me}_5)\text{W}(\text{O})_2\text{Ru}_3(\mu_3\text{-NPh})(\text{CCMe}=\text{CH}_2)(\text{CO})_8$ (**7**), which are generated by removal of the vinyl or the dioxo tungsten fragment from the coordination sphere of ruthenium metal, respectively. In addition, upon exposure to pressurized CO atmosphere, complex **7** slowly converts to $\text{Ru}_3(\text{CO})_9[\text{C}_6\text{H}_5\text{O}(\text{CONHPh})]$ (**8**), which has been crystallographically shown to possess a Ru_3 skeleton with the vinylacetylide linked with one bridging CO and a carboxamido fragment; the latter is derived from the coupling of CO with the imido group. A possible reaction mechanism leading to the formation of **8** is discussed.

Transition metal carbonyl acetylide complexes $\text{L}_m\text{M}-\text{C}\equiv\text{CR}$ are potential building blocks for higher nuclearity cluster compounds with interesting structural properties and diversified reactivities.¹ For example, the acetylide-bridged trinuclear complexes $\text{CpMCo}_2(\text{CCR})(\text{CO})_8$ can be constructed by linking of $\text{CpM}(\text{CO})_2(\text{CCR})$, $\text{M} = \text{Fe}, \text{Ru}$; $\text{R} = \text{Me}, \text{Ph}, \text{Bu}^t$, with $\text{Co}_2(\text{CO})_8$.² In these complexes the acetylide underwent rapid

reaction with oxygen, which resulted in the formation of the alkyldiene-bridged clusters $\text{CpMCo}_2(\mu_3\text{-CR})(\text{CO})_7$. In addition, a variety of polymetallic ethynyl complexes were prepared by structure expansion reactions using the parent acetylide complex $(\text{C}_5\text{Me}_5)\text{Fe}(\text{CO})_2(\text{CCH})$,³ which provided a good model for surface-bound C_2 species formed during catalytic CO hydrogenation. Recently, Chi and co-workers have synthesized the trinuclear clusters $\text{LWRu}_2(\text{CCPh})(\text{CO})_8$ or the corresponding tetrametallic clusters $\text{LWOS}_3(\text{CCPh})(\text{CO})_{11}$ by condensation of $\text{LW}(\text{CO})_3(\text{CCPh})$, $\text{L} = \text{Cp}$ and C_5Me_5 , with $\text{Ru}_3(\text{CO})_{12}$ or with the heavier congener $\text{Os}_3(\text{CO})_{10}(\text{NCMe})_2$, respectively.⁴ In these complexes, the ligated

[†] National Tsing Hua University.

[‡] Steacie Institute for Molecular Sciences.

[§] National Taiwan University.

(1) (a) Yasufuku, K.; Aoki, K.; Yamazaki, H. *Bull. Chem. Soc. Jpn.* **1975**, *48*, 1616. (b) Koridze, A. A.; Kizas, O. A.; Kolobova, N. E.; Vinogradova, V. N.; Ustynuk, N. A.; Petrovskii, P. V.; Yanovsky, A. I.; Struchkov, Y. T. *J. Chem. Soc., Chem. Commun.* **1984**, 1158. (c) Bruce, M. I.; Duffy, D. N.; Humphrey, M. G. *Aust. J. Chem.* **1986**, *39*, 159. (d) Chi, Y.; Lee, G.-H.; Peng, S.-M.; Wu, C.-H. *Organometallics* **1989**, *8*, 1574. (e) Cheng, P.-S.; Chi, Y.; Peng, S.-M.; Lee, G.-H. *Organometallics* **1993**, *12*, 250. (f) Tseng, W.-C.; Chi, Y.; Su, C.-J.; Carty, A. J.; Peng, S.-M.; Lee, G.-H. *J. Chem. Soc., Dalton Trans.* **1998**, 1053.

(2) (a) Bernhardt, W.; Vahrenkamp, H. *Organometallics* **1986**, *5*, 2388. (b) Bernhardt, W.; Vahrenkamp, H. *J. Organomet. Chem.* **1990**, *383*, 357.

(3) (a) Akita, M.; Terada, M.; Moro-oka, Y. *Organometallics* **1992**, *11*, 1825. (b) Akita, M.; Hirakawa, H.; Sakaki, K.; Moro-oka, Y. *Organometallics* **1995**, *14*, 2775. (c) Akita, M.; Moro-oka, Y. *Bull. Chem. Soc. Jpn.* **1995**, *68*, 420. (d) Akita, M.; Ishii, N.; Takabuchi, A.; Tanaka, M.; Moro-oka, Y. *Organometallics* **1994**, *13*, 258.

(4) (a) Chi, Y.; Lee, G.-H.; Peng, S.-M.; Liu, B.-J. *Polyhedron* **1989**, *8*, 2003. (b) Chi, Y.; Wu, C.-H.; Peng, S.-M.; Lee, G.-H. *Organometallics* **1990**, *9*, 2305. (c) Hwang, D.-K.; Chi, Y.; Peng, S.-M.; Lee, G.-H. *Organometallics* **1990**, *9*, 2709.

acetylide converts to a carbide plus an alkylidyne ligand during the subsequent reactivity studies, thus furnishing a novel example of reversible scission of acetylide C–C bond.⁵

It is notable that each of the above-mentioned acetylide complexes contains a low-valent metal atom with at least two CO ligands. Thus the acetylide complexes can react with other low-valent organometallics to form relatively strong metal–metal bonding, through a facile CO elimination process. Naturally, it is of interest to compare such reactivity patterns with that of the acetylide complexes bearing a high oxidation state metal atom. One target suitable for such study is the complex with the general formula $(C_5Me_5)W(O)_2(CCR)$,⁶ in which the tungsten atom is at the formal oxidation state of +6 having two π -donor oxo ligands. We then proceeded to examine the cluster-building reactions of $(C_5Me_5)W(O)_2(CCR)$ with polymetallic cluster compounds such as $Os_3(CO)_{10}(NCMe)_2$,⁷ $Ru_4(\mu_3-PPh)(CO)_{14}$,⁸ or $Ru_6(\mu_6-C)(CO)_{17}$,⁹ with the objective of preparing complexes that contain an dioxo tungsten unit directly bound to the low-valent metal carbonyl framework. In this paper, we describe the reactions of $(C_5Me_5)W(O)_2(CCR)$, R = Ph and $CMe=CH_2$, with the corresponding imido cluster $Ru_3(\mu_3-NPh)(CO)_{10}$. We intend to use the reactivity obtained from this new system to further demonstrate the versatile bonding capability of the dioxo tungsten moiety within this class of high–low oxidation state complexes and to interpret the inherent property of the acetylide substituent R.

Experimental Section

General Information and Materials. Infrared spectra were recorded on a Perkin-Elmer 2000 FT-IR spectrometer. ¹H and ¹³C NMR spectra were recorded on a Bruker AM-400 or a AMX-300 instrument. Mass spectra were obtained on a JEOL SX-102A instrument operating in fast atom bombardment (FAB) mode. All reactions were performed under a nitrogen atmosphere using dried solvents. The imido cluster complex $Ru_3(\mu_3-NPh)(CO)_{10}$ was prepared from the reaction of $Ru_3(CO)_{12}$ with nitrosobenzene in THF solution.¹⁰ The dioxo acetylide complexes $(C_5Me_5)W(O)_2(CCR)$, R = Ph and $CMe=CH_2$, were prepared by oxidation of $(C_5Me_5)W(CO)_3(CCR)$ using a 30% solution of H_2O_2 , followed by treatment with PPh_3 .⁶ The reactions were monitored by analytical thin-layer chromatography (5735 Kieselgel 60 F₂₅₄, E. Merck), and the products were separated on commercially available preparative thin-layer chromatographic plates (Kieselgel 60 F₂₅₄, E. Merck). Elemental analyses were performed at the NSC Regional Instrumentation Center at National Cheng Kung University, Tainan, Taiwan.

Condensation of $Ru_3(\mu_3-NPh)(CO)_{10}$ with $(C_5Me_5)W(O)_2(CCR)$. A toluene solution (40 mL) of $Ru_3(\mu_3-NPh)(CO)_{10}$ (68 mg, 0.101 mmol) and $(C_5Me_5)W(O)_2(CCR)$ (45 mg, 0.100 mmol) was refluxed under nitrogen for 1 h, during which

period the color changed from yellow to red-brown. After allowing the solution to cool to room temperature, the solvent was removed, and the residue was dissolved in a minimum amount of CH_2Cl_2 and separated by thin-layer chromatography (CH_2Cl_2 /hexane = 2:1), giving 77 mg of $(C_5Me_5)W(O)(\mu-O)Ru_3(\mu_3-NPh)(CCPh)(CO)_8$ (**1a**, 0.071 mmol, 71%) and 6 mg of $(C_5Me_5)W(O)(\mu-O)Ru_4(\mu_3-NPh)(CCPh)(CO)_{10}$ (**2**, 0.005 mmol, 5%). Crystals of **1a** suitable for X-ray diffraction study were obtained from a layered solution of CH_2Cl_2 and methanol.

Spectral data for **1a** are as follows. MS (FAB, ¹⁸⁴W, ¹⁰²Ru): m/z 1073 (M^+). IR (C_6H_{12}): $\nu(CO)$, 2081 (m), 2064 (vs), 2041 (s), 2010 (s), 2004 (s), 1987 (s), 1957 (br, w) cm^{-1} . ¹H NMR (300 MHz, $CDCl_3$, 293 K): δ 7.86 (d, 2H, $J_{HH} = 7.5$ Hz), 7.48 (t, 2H, $J_{HH} = 7.5$ Hz), 7.34 (t, 1H, $J_{HH} = 7.5$ Hz), 7.11–7.04 (m, 4H), 6.90–6.84 (m, 1H), 2.06 (s, 15H). ¹³C NMR (75 MHz, $CDCl_3$, 293 K): CO δ 198.7, 196.8, 196.1, 195.5, 193.0, 191.5, 190.9, 187.7; δ 171.8 (1C, $J_{WC} = 167$ Hz), 169.0 (1C, *i*- C_6H_5), 144.5 (1C, *i*- C_6H_5), 128.9 (2C, C_6H_5), 128.3 (2C, C_6H_5), 128.2 (2C, C_6H_5), 126.7 (1C, *p*- C_6H_5), 123.7 (2C, C_6H_5), 123.6 (1C, *p*- C_6H_5), 117.7 (C_5Me_5), 76.2 (1C), 11.4 (C_5Me_5). Anal. Calcd for $C_{32}H_{25}O_{10}NRu_3W \cdot 1/2CH_2Cl_2$: C, 35.07; H, 2.35; N, 1.26. Found: C, 34.95; H, 2.72; N, 1.31.

Spectral data for **2** are as follows. MS (FAB, ¹⁸⁴W, ¹⁰²Ru): m/z 1231 (M^+). IR (C_6H_{12}): $\nu(CO)$, 2072 (m), 2052 (vs), 2039 (vs), 2024 (vs), 2006 (s), 1994 (w), 1973 (s), 1959 (m), 1892 (m), 1838 (s) cm^{-1} . ¹H NMR (400 MHz, $CDCl_3$, 293 K): δ 7.11–7.05 (m, 3H), 6.93 (br, 1H), 6.70 (t, 2H, $J_{HH} = 7.6$ Hz), 5.55 (t, 2H, $J_{HH} = 7.6$ Hz), 5.66 (br, 2H), 1.90 (s, 15H). Anal. Calcd for $C_{34}H_{25}O_{12}NRu_4W$: C, 33.26; H, 2.05; N, 1.14. Found: C, 33.45; H, 2.14; N, 1.14.

Preparation of **2.** A toluene solution (40 mL) of **1a** (61 mg, 0.057 mmol) and $Ru_3(CO)_{12}$ (72 mg, 0.113 mmol) was refluxed under nitrogen for 2 h, during which period the color changed from orange to dark-brown. After the solvent was removed under vacuum, the residue was purified by thin-layer chromatography (CH_2Cl_2 /hexane = 1:1) and recrystallized from a mixed solution of CH_2Cl_2 and methanol; 33 mg of **2** (0.027 mmol, 47%) was produced as a brown crystalline material.

Reaction of **2 with CO.** A toluene solution (40 mL) of **2** (27 mg, 0.022 mmol) was heated at 60 °C under carbon monoxide for 5 min, during which period the color changed from dark-red to orange. After the removal of solvent in vacuo, the residue was redissolved in CH_2Cl_2 and separated by TLC (CH_2Cl_2 /hexane = 1:1), giving 21 mg of **1a** (0.019 mmol, 86%).

Reaction of $Ru_3(\mu_3-NPh)(CO)_{10}$ and $(C_5Me_5)W(O)_2(CCR)$. A toluene solution (40 mL) of $(C_5Me_5)W(O)_2(CCR)$ (68 mg, 0.163 mmol) and $Ru_3(\mu_3-NPh)(CO)_{10}$ (110 mg, 0.163 mmol) was refluxed under nitrogen for 1 h, during which period the color changed from yellow to red-brown. After removal of solvent, the residue was dissolved in a minimum amount of CH_2Cl_2 and separated by thin-layer chromatography (CH_2Cl_2 /hexane = 2:1), giving 24 mg of red $(C_5Me_5)W(\mu-O)_2Ru_3(\mu_3-NPh)(CCCMe=CH_2)(CO)_6$ (**4**, 0.025 mmol, 15%) and 76 mg of orange $(C_5Me_5)W(O)(\mu-O)Ru_3(\mu_3-NPh)(CCCMe=CH_2)(CO)_8$ (**1b**, 0.073 mmol, 45%). Crystals of complexes **1b** and **4** were obtained from a layered solution of CH_2Cl_2 and methanol.

Spectral data for **1b** are as follows. MS (FAB, ¹⁸⁴W, ¹⁰²Ru): m/z 1009 ($M^+ - CO$). IR (C_6H_{12}): $\nu(CO)$, 2081 (m), 2063 (vs), 2041 (s), 2009 (s), 2003 (s), 1987 (s), 1956 (br, w) cm^{-1} . ¹H NMR (400 MHz, $CDCl_3$, 293K) δ 7.08–7.00 (m, 4H), 6.66 (t, 1H, $J_{HH} = 6.8$ Hz), 5.65 (s, 1H), 5.39 (s, 1H), 2.16 (s, 3H), 2.15 (s, 15H). ¹³C NMR (100 MHz, $CDCl_3$, 293 K): CO δ 198.5, 197.0, 196.2, 195.4, 193.1, 192.5, 191.5, 187.7; δ 171.1 (1C, $J_{WC} = 168$ Hz), 169.3 (1C, *i*- C_6H_5), 146.9 ($CMe=CH_2$), 128.2 (2C, C_6H_5), 123.7 (2C, C_6H_5), 123.6 (1C, *p*- C_6H_5), 117.6 (C_5Me_5), 116.7 ($CMe=CH_2$), 82.4 (1C), 23.0 (Me), 11.4 (C_5Me_5). Anal. Calcd for $C_{29}H_{25}O_{10}NRu_3W$: C, 33.67; H, 2.44; N 1.35. Found: C, 33.66; H, 2.39; N 1.37.

Spectral data for **4** are as follows. MS (FAB, ¹⁸⁴W, ¹⁰²Ru): m/z 981 (M^+). IR (C_6H_{12}): $\nu(CO)$, 2044 (s), 2008 (vs), 1965 (vw),

(5) (a) Chiang, S.-J.; Chi, Y.; Su, P.-C.; Peng, S.-M.; Lee, G.-H. *J. Am. Chem. Soc.* **1994**, *116*, 11181. (b) Chi, Y.; Su, P.-C.; Peng, S.-M.; Lee, G.-H. *Organometallics* **1995**, *14*, 5483. (c) Chi, Y.; Chung, C.; Chou, Y.-C.; Su, P.-C.; Chiang, S.-J.; Peng, S.-M.; Lee, G.-H. *Organometallics* **1997**, *16*, 1702.

(6) Shiu, C.-W.; Su, C.-J.; Pin, C.-W.; Chi, Y.; Peng, S.-M.; Lee, G.-H. *J. Organomet. Chem.* **1997**, *545–546*, 151.

(7) Shiu, C.-W.; Chi, Y.; Carty, A. J.; Peng, S.-M.; Lee, G.-H. *Organometallics* **1997**, *16*, 5368.

(8) Blenkiron, P.; Carty, A. J.; Peng, S.-M.; Lee, G.-H.; Su, C.-J.; Shiu, C.-W.; Chi, Y. *Organometallics* **1997**, *16*, 519.

(9) Chao, W.-J.; Chi, Y.; Chung, C.; Carty, A. J.; Delgado, E.; Peng, S.-M.; Lee, G.-H. *J. Organomet. Chem.*, in press.

(10) Smieja, J. A.; Gladfelter, W. L. *Inorg. Chem.* **1986**, *25*, 2667.

1956 (w), 1940 (m) cm^{-1} . ^1H NMR (400 MHz, CDCl_3 , 293 K): δ 6.87 (t, 2H, $J_{\text{HH}} = 7.4$ Hz), 6.71 (t, 1H, $J_{\text{HH}} = 7.4$ Hz), 6.44 (d, 2H, $J_{\text{HH}} = 7.4$ Hz), 4.09 (s, 1H), 3.55 (s, 1H), 2.42 (s, 3H), 2.33 (s, 15H). ^{13}C NMR (100 MHz, CDCl_3 , 293 K): CO δ 198.0, 197.9, 197.7 (2CO), 196.1, 194.7; δ 167.3 (1C, *i*- C_6H_5), 160.2 (1C, $J_{\text{WC}} = 37$ Hz), 139.5 (1C, $J_{\text{WC}} = 186$ Hz), 127.7 (2C, C_6H_5), 122.8 (1C, *p*- C_6H_5), 119.7 (2C, C_6H_5), 116.6 (C_5Me_5), 84.0 ($\text{CMe}=\text{CH}_2$), 49.9 ($\text{CMe}=\text{CH}_2$), 26.2 (Me), 11.1 (C_5Me_5). Anal. Calcd for $\text{C}_{27}\text{H}_{25}\text{O}_9\text{NRu}_3\text{W}$: C, 33.14; H, 2.58; N, 1.43. Found: C, 33.24; H, 2.59; N, 1.47.

Reaction of 4 with PMe_2Ph . A toluene solution (30 mL) of **4** (100 mg, 0.102 mmol) and PMe_2Ph (15 μL , 0.105 mmol) was heated to reflux under nitrogen for 1 h, during which time the color changed gradually from red to red-brown. After removal of the solvent in vacuo, the residue was dissolved in a minimum amount of CH_2Cl_2 and separated by TLC ($\text{CH}_2\text{Cl}_2/\text{hexane} = 3:1$), giving 44 mg of dark-red (C_5Me_5) $\text{W}(\mu\text{-O})_2\text{-Ru}_3(\text{CCCMe}=\text{CH}_2)(\mu_3\text{-NPh})(\text{CO})_5(\text{PMe}_2\text{Ph})$ (**5**, 0.04 mmol, 40%), which was further purified by recrystallization from CH_2Cl_2 and hexane at room temperature.

Spectral data for **5** are as follows. MS (FAB, ^{184}W , ^{102}Ru): m/z 1091 (M^+). IR (C_6H_{12}): $\nu(\text{CO})$, 2005 (w), 1990 (vs, br), 1972 (vw), 1938 (sh, w), 1928 (s, br) cm^{-1} . ^1H NMR (400 MHz, CDCl_3 , 293 K): δ 7.65 (dd, 2H, $J_{\text{HH}} = 7.2$ Hz, $J_{\text{PH}} = 11.2$ Hz), 7.50 (m, 2H, $J_{\text{HH}} = 7.2$ Hz, $J_{\text{PH}} = 1.7$ Hz), 7.42 (m, 1H, $J_{\text{HH}} = 7.2$ Hz, $J_{\text{PH}} = 1.6$ Hz), 6.80 (t, 2H, $J_{\text{HH}} = 7.6$ Hz), 6.64 (t, 1H, $J_{\text{HH}} = 7.6$ Hz), 6.23 (d, 2H, $J_{\text{HH}} = 7.6$ Hz), 3.21 (s, 1H), 2.87 (d, 1H, $J_{\text{PH}} = 4.8$ Hz), 2.29 (s, 15H), 2.24 (s, 3H), 1.70 (d, 3H, $J_{\text{PH}} = 9.4$ Hz), 1.60 (d, 3H, $J_{\text{PH}} = 9.2$ Hz). ^{13}C NMR (100 MHz, CDCl_3 , 293 K): CO δ 202.1, 201.5 ($J_{\text{PC}} = 16$ Hz), 199.9, 199.8, 195.4; δ 167.2 (1C, NC_6H_5), 159.5 (1C, $J_{\text{WC}} = 37$ Hz, $J_{\text{PC}} = 10$ Hz), 141.2 (1C, PC_6H_5 , $J_{\text{PC}} = 47$ Hz), 140.7 (1C, $J_{\text{WC}} = 184$ Hz, $J_{\text{PC}} = 3$ Hz), 129.3 (1C, PC_6H_5), 128.9 (2C, C_6H_5 , $J_{\text{PC}} = 9$ Hz), 128.7 (2C, PC_6H_5 , $J_{\text{PC}} = 10$ Hz), 127.6 (2C, NC_6H_5), 121.6 (2C, NC_6H_5), 121.5 (1C, NC_6H_5), 115.8 (C_5Me_5), 80.6 ($\text{CMe}=\text{CH}_2$), 49.2 ($\text{CMe}=\text{CH}_2$), 26.7 (Me), 18.3 (Me, $J_{\text{PC}} = 29$ Hz), 16.2 (Me, $J_{\text{PC}} = 28$ Hz), 11.2 (C_5Me_5). Anal. Calcd for $\text{C}_{29}\text{H}_{25}\text{O}_{10}\text{-NPRu}_3\text{W-CH}_2\text{Cl}_2$: C, 35.82; H, 3.26; N 1.19. Found: C, 35.65; H, 3.33; N 1.21.

Thermolysis of 1b. A toluene solution (60 mL) of **1b** (85 mg, 0.082 mmol) was refluxed under nitrogen for 1 h, during which period the color changed from red to red-brown. After the solvent was removed under vacuum, the residue was purified by thin-layer chromatography ($\text{CH}_2\text{Cl}_2/\text{hexane} = 2:1$) to afford 60 mg of the dark-red **4** (0.062 mmol, 75%).

Reaction of 4 with CO. A toluene solution (30 mL) of **4** (80 mg, 0.082 mmol) was heated to reflux under CO for 5 min, during which the color changed from red to orange. After removal of solvent, the residue was redissolved in CH_2Cl_2 and separated by thin-layer chromatography (dichloromethane/hexane = 2:1), affording 80 mg of **1b** (0.077 mmol, 94%).

Reaction of 4 with CO at Room Temperature. A toluene solution (30 mL) of **4** (80 mg, 0.082 mmol) was stirred under CO atmosphere for 30 min, during which time the color changed from red to red-orange. After removal of solvent, the residue was redissolved in CH_2Cl_2 and separated by thin-layer chromatography (dichloromethane/hexane = 2:1), affording 21 mg of dark-red (C_5Me_5) $\text{W}(\mu\text{-O})_2\text{-Ru}_3(\mu_3\text{-NPh})(\text{CCCMe}=\text{CH}_2)(\text{CO})_7$ (**6**) (0.021 mmol, 34%), 20 mg of **1b** (0.019 mmol, 34%), and 14 mg of orange (C_5Me_5) $\text{W}(\text{O})_2\text{-Ru}_3(\mu_3\text{-NPh})(\text{CCCMe}=\text{CH}_2)(\text{CO})_8$ (**7**) (0.014 mmol, 23%). Crystals of **7** suitable for X-ray diffraction study were obtained from a layered solution of CH_2Cl_2 and methanol.

Spectral data for **6** are as follows. MS (FAB, ^{184}W , ^{102}Ru): m/z 1009 (M^+). IR (C_6H_{12}): $\nu(\text{CO})$, 2074 (s), 2024 (vs), 2010 (vs), 1960 (m), 1949 (m) cm^{-1} . ^1H NMR (400 MHz, CDCl_3 , 293 K): δ 6.76 (t, 2H, $J_{\text{HH}} = 7.6$ Hz), 6.63 (t, 1H, $J_{\text{HH}} = 7.6$ Hz), 6.26 (d, 2H, $J_{\text{HH}} = 7.6$ Hz), 5.42 (s, 1H), 5.23 (s, 1H), 2.28 (s, 3H), 2.25 (s, 15H). ^{13}C NMR (100 MHz, CDCl_3 , 293 K): CO δ 197.0 (2CO), 196.4 (2CO), 194.7 (3CO); δ 182.7 (1C, $J_{\text{WC}} = 33$ Hz), 167.1 (1C, *i*- C_6H_5), 159.4 (1C, $J_{\text{WC}} = 174$ Hz), 150.1 ($\text{CMe}=\text{CH}_2$), 127.9 (2C, C_6H_5), 122.6 (1C, *p*- C_6H_5), 120.3 (2C, C_6H_5), 117.6 ($\text{CMe}=\text{CH}_2$), 116.5 (C_5Me_5), 26.7 (Me), 11.1 (C_5Me_5). Anal. Calcd for $\text{C}_{28}\text{H}_{25}\text{O}_9\text{NRu}_3\text{W}$: C, 33.41; H, 2.50; N, 1.39. Found: C, 33.59; H, 2.62; N, 1.46.

Spectral data for **7** are as follows. MS (FAB, ^{184}W , ^{102}Ru): m/z 1037 (M^+). IR (CH_2Cl_2): $\nu(\text{CO})$, 2084 (w), 2064 (vs), 2024 (vs), 2007 (s), 1979 (m), 1952 (w) cm^{-1} . ^1H NMR (400 MHz, CDCl_3 , 293 K): δ 6.99 (t, 2H, $J_{\text{HH}} = 7.2$ Hz), 6.88 (d, 2H, $J_{\text{HH}} = 7.2$ Hz), 6.78 (d, 1H, $J_{\text{HH}} = 7.2$ Hz), 4.01 (s, 1H), 3.46 (s, 1H), 2.28 (s, 3H), 2.20 (s, 15H). ^{13}C NMR (100 MHz, CDCl_3 , 293 K): CO δ 199.2, 196.5 (2CO), 196.1, 192.7, 191.6, 190.0, 189.5; δ 167.2 (1C, *i*- C_6H_5), 136.1 (1C, $J_{\text{WC}} = 26$ Hz), 128.2 (2C, C_6H_5), 123.8 (2C, C_6H_5), 123.4 (1C, *p*- C_6H_5), 118.4 (C_5Me_5), 70.3 ($\text{CMe}=\text{CH}_2$), 55.3 (1C, $J_{\text{WC}} = 220$ Hz), 48.2 ($\text{CMe}=\text{CH}_2$), 26.5 (Me), 11.0 (C_5Me_5). Anal. Calcd for $\text{C}_{29}\text{H}_{25}\text{O}_{10}\text{-NRu}_3\text{W}$: C, 33.67; H, 2.44; N, 1.35. Found: C, 33.67; H, 2.52; N, 1.41.

Thermolysis of 6. A toluene solution (30 mL) of **6** (65 mg, 0.064 mmol) was refluxed for 20 min, during which the color changed from red-brown to red. After removal of solvent, the residue was redissolved in CH_2Cl_2 and separated by thin-layer chromatography (dichloromethane/hexane = 2:1), affording 58 mg of **4** (0.059 mmol, 92%).

Reaction of 6 with CO. A toluene solution (30 mL) of **6** (50 mg, 0.05 mmol) was refluxed under CO atmosphere for 5 min, during which the color changed from red to orange. After removal of solvent, the residue was redissolved in CH_2Cl_2 and separated by thin-layer chromatography (dichloromethane/hexane = 2:1), affording 48 mg of **1b** (0.046 mmol, 92%).

Reaction of 7 with CO. A toluene solution (30 mL) of **7** (150 mg, 0.145 mmol) was stirred under CO atmosphere (40 psi) at 30 $^\circ\text{C}$ and for 24 h, during which time the color changed from light yellow to yellow. After removal of solvent, the residue was separated by thin-layer chromatography using pure CH_2Cl_2 as eluent, affording 66 mg of yellow-orange $\text{Ru}_3(\text{CO})_9(\text{C}_6\text{H}_5\text{O}(\text{CONHPh}))$ (**8**) (0.086 mmol, 59%), 6.5 mg of **1b** (0.006 mmol, 4%), and 20 mg of unreacted **7**. Single crystals suitable for X-ray analysis were obtained from a solution of dichloromethane and methanol.

Spectral data for **8** are as follows. MS (FAB, ^{102}Ru): m/z 771 (M^+). IR (C_6H_{12}): $\nu(\text{CO})$, 2099 (m), 2075 (s), 2038 (s), 2022 (s), 2011 (m), 1986 (w), 1967 (sh, w), 1910 (br, w) cm^{-1} . ^1H NMR (400 MHz, CDCl_3 , 293 K): δ 10.23 (s, 1H), 7.21 (t, $J_{\text{H-H}} = 7.2$ Hz, 2H), 7.08 (d, $J_{\text{H-H}} = 7.2$ Hz, 3H), 3.85 (s, 1H), 2.31 (s, 1H), 2.22 (s, 3H). ^{13}C NMR (75 MHz, CDCl_3 , 293 K): CO, δ 220.9, 218.0, 202.1, 201.2, 194.9, 194.3, 191.9, 191.8, 190.7 (2C), 173.6; δ 160.4, 136.2 (*i*- C_6H_5), 129.0 (2C, *o*- C_6H_5), 125.2 (*p*- C_6H_5), 120.1 (2C, *m*- C_6H_5), 114.6, 54.9, 46.9 (CH_2), 30.5 (Me). Anal. Calcd for $\text{C}_{22}\text{H}_{11}\text{O}_4\text{NRu}_3$: C, 34.38; H, 1.44; N, 1.82. Found: C, 34.78; H, 1.57; N, 1.79.

X-ray Crystallography. The X-ray diffraction measurements were carried out on a Nonius CAD-4 diffractometer at room temperature. For all experiments, the lattice parameters were determined from 25 randomly selected high-angle reflections. Three standard reflections were monitored every 3600 s. No significant change in intensities ($\leq 2\%$) was observed during the course of all data collection. Intensities of the diffraction signals were corrected for Lorentz, polarization, and absorption effects (ψ scans). The structure was solved by using the NRCC-SDP-VAX package. All the non-hydrogen atoms had anisotropic temperature factors, while the hydrogen atoms of the organic substituents were placed at the calculated positions with $U_{\text{H}} = U_{\text{C}} + 0.1$. The crystallographic refinement parameters of complexes **1a**, **5**, **7**, and **8** are given in Table 1, while their selected bond distances and angles are presented in Tables 2–5, respectively.

Results and Discussion

Condensation of $\text{Ru}_3(\mu_3\text{-NPh})(\text{CO})_{10}$ with ($\text{C}_5\text{-Me}_5$) $\text{W}(\text{O})_2(\text{CCPh})$. When a toluene solution of $\text{Ru}_3(\mu_3\text{-$

Table 1. Experimental Data for the X-ray Diffraction Studies of 1a, 5, 7, and 8^a

	1a	5	7	8
formula	C ₃₂ H ₂₅ NO ₁₀ Ru ₃ W	C ₃₄ H ₃₆ NO ₇ PRu ₃ W·CH ₂ Cl ₂	C ₂₉ H ₂₅ NO ₁₀ Ru ₃ W	C ₂₂ H ₁₁ NO ₁₁ Ru ₃
mol wt	1070.60	1173.62	1034.57	768.54
crystal system	monoclinic, <i>P</i> ₂ ₁ / <i>n</i>	triclinic, <i>P</i> $\bar{1}$	monoclinic, <i>P</i> ₂ ₁ / <i>n</i>	monoclinic, <i>P</i> ₂ ₁ / <i>c</i>
<i>a</i> (Å)	11.341(1)	10.798(3)	9.255(3)	8.2229(8)
<i>b</i> (Å)	15.033(2)	13.056(2)	25.372(4)	17.169(1)
<i>c</i> (Å)	20.765(2)	14.200(2)	13.639(3)	17.132(2)
α (deg)		93.68(1)		
β (deg)	105.169(8)	98.78(2)	95.93(2)	103.369(8)
γ (deg)		92.01(2)		
<i>U</i> (Å ³)	3416.9(7)	1972.3(6)	3186(1)	2353.1(4)
<i>Z</i>	4	2	4	4
<i>D</i> _c (g/cm ³)	2.081	1.976	2.157	2.169
<i>F</i> (000)	2019	1122	1947	1480
crystal size, mm	0.25 × 0.35 × 0.60	0.30 × 0.40 × 0.40	0.08 × 0.35 × 0.35	0.35 × 0.25 × 0.20
<i>h, k, l</i> ranges	-14 to +14, 0-19, 0-26	-12 to +12, 0-15, -16-16	-9 to +9, 0-13, -15-15	-10 to +9, 0-20, 0-21
μ (cm ⁻¹)	47.76	41.67	51.0	19.27
trans. factors; max, min	0.718, 1.000	0.631, 1.000	0.472, 1.000	0.600, 0.654
no. of unique data (<i>2</i> θ _{max} (deg))	7841 (55)	6929 (50)	5589 (50)	4590 (52)
data with <i>I</i> > 2 σ (<i>I</i>)	5545	5809	4154	3708
no. of parameters	425	452	398	335
weight modifier, <i>g</i>	0.0001	0.0001	0.00005	0.0001
maximum Δ/σ ratio	0.009	0.003	0.0002	0.0017
<i>R</i> , <i>R</i> _w	0.030; 0.030	0.026; 0.026	0.031; 0.032	0.025; 0.027
GOF	1.31	1.64	1.41	1.38
residual e-density, e/Å ³	-0.78/0.69	-0.91/1.21	-0.96/1.07	-0.45/0.38

^a Features common to all determinations: temperature = 297 K, λ (Mo K α) = 0.709 30 Å; minimize function $\sum(w|F_o - F_c|^2)$, weighting scheme $w^{-1} = \sigma^2(F_o) + |g|F_o^2$; GOF = $[\sum w|F_o - F_c|^2 / (N_o - N_v)]^{1/2}$ (*N*_o = number of observations; *N*_v = number of variables).

Table 2. Selected Bond Distances (Å) and Angles (deg) of 1a (esd in Parentheses)

W-Ru(1)	2.7854(6)	Ru(1)-Ru(2)	2.8708(7)
Ru(1)-Ru(3)	2.7154(6)	Ru(2)···Ru(3)	3.2330(7)
Ru(1)-N	2.049(4)	Ru(2)-N	2.066(4)
Ru(3)-N	2.081(4)	W-O(9)	1.796(4)
Ru(1)-O(9)	2.182(4)	W-O(10)	1.724(4)
W-C(9)	2.070(5)	Ru(1)-C(9)	2.140(5)
Ru(3)-C(9)	2.350(5)	Ru(2)-C(10)	2.126(5)
Ru(3)-C(10)	2.264(5)	C(9)-C(10)	1.352(7)
\angle O(9)-W-O(10)	107.8(2)	\angle C(9)-W-O(9)	101.1(2)
\angle C(9)-W-O(10)	103.1(2)		

Table 3. Selected Bond Distances (Å) and Angles (deg) of 5 (esd in Parentheses)

W-Ru(1)	2.8057(6)	W-Ru(2)	2.8378(6)
Ru(1)···Ru(2)	3.2927(7)	Ru(1)-Ru(3)	2.7618(7)
Ru(2)-Ru(3)	2.7543(7)	Ru(1)-N	2.099(4)
Ru(2)-N	2.135(4)	Ru(3)-N	2.058(4)
W-O(6)	1.809(3)	Ru(1)-O(6)	2.133(3)
W-O(7)	1.797(3)	Ru(2)-O(7)	2.218(3)
W-C(6)	1.956(5)	Ru(1)-C(6)	2.222(5)
Ru(2)-C(6)	2.219(4)	Ru(2)-C(7)	2.177(5)
Ru(3)-C(7)	2.122(4)	Ru(3)-C(8)	2.231(5)
Ru(3)-C(9)	2.237(6)	Ru(3)-P	2.366(1)
C(6)-C(7)	1.347(7)	C(7)-C(8)	1.423(7)
C(8)-C(9)	1.410(7)	C(8)-C(10)	1.499(8)
\angle O(6)-W-O(7)	105.3(6)	\angle C(6)-W-O(6)	100.9(2)
\angle C(6)-W-O(7)	102.5(2)		

Table 4. Selected Bond Distances (Å) and Angles (deg) of 7 (esd in Parentheses)

Ru(1)···Ru(2)	3.249(1)	Ru(1)-Ru(3)	2.7161(9)
Ru(2)-Ru(3)	2.782(1)	Ru(1)-N	2.106(5)
Ru(2)-N	2.061(5)	Ru(3)-N	2.077(5)
W-O(9)	1.715(5)	W-O(10)	1.703(6)
W-C(9)	2.090(7)	Ru(1)-C(9)	2.290(6)
Ru(2)-C(9)	2.249(6)	Ru(1)-C(10)	2.292(6)
Ru(2)-C(10)	2.468(6)	Ru(3)-C(10)	2.126(7)
Ru(3)-C(11)	2.214(7)	Ru(3)-C(12)	2.270(7)
C(9)-C(10)	1.34(1)	C(10)-C(11)	1.440(9)
C(11)-C(12)	1.41(1)		
\angle O(9)-W-O(10)	106.8(4)	\angle C(9)-W-O(9)	100.3(3)
\angle C(9)-W-O(10)	101.2(3)		

Table 5. Selected Bond Distances (Å) of 8 (esd in Parentheses)

Ru(1)-Ru(2)	2.8054(5)	Ru(2)-Ru(3)	2.8164(5)
Ru(1)-C(10)	2.243(4)	Ru(1)-C(11)	2.374(4)
Ru(1)-C(15)	2.089(4)	Ru(2)-C(5)	1.850(4)
Ru(2)-C(13)	1.988(3)	Ru(2)-C(14)	2.109(3)
Ru(3)-C(5)	2.391(4)	Ru(3)-C(13)	2.024(3)
Ru(3)-O(10)	2.127(2)	C(10)-C(11)	1.306(5)
C(11)-C(12)	1.506(5)	C(11)-C(13)	1.407(5)
C(13)-C(14)	1.477(5)	C(14)-C(15)	1.457(5)
C(15)-O(11)	1.216(4)	C(16)-O(10)	1.255(4)
C(16)-N(1)	1.334(4)		

The molecular structure of **1a** was established by a single-crystal X-ray diffraction study. As indicated in Figure 1, the molecule consists of an open triangular arrangement of three ruthenium atoms with two short Ru-Ru distances, Ru(1)-Ru(2) = 2.8708(7) Å and Ru(1)-Ru(3) = 2.7154(6) Å, and a third, much longer Ru-Ru distance, Ru(2)···Ru(3) = 3.2330(7) Å. The Ru(2) and Ru(3) atoms each carries three terminal CO ligands, while the Ru(1) atom possesses only two CO ligands. In addition, the Ru₃ metal framework is further coordinated by a triply bridging imido ligand with three nearly identical Ru-N distances in the range 2.049(4)-2.081(4) Å and by a bridging acetylide ligand on the opposite side of the Ru₃ plane. The bonding features of

NPh)(CO)₁₀ and stoichiometric amount of (C₅Me₅)W(O)₂(CCPh) was heated to reflux for 1 h, an orange-red tetrametallic complex (**1a**) with the formula (C₅Me₅)W(O)(μ -O)Ru₃(μ ₃-NPh)(CCPh)(CO)₈ was obtained in 71% yield, together with small amounts of a brown, pentametallic complex (C₅Me₅)W(O)(μ -O)Ru₄(μ ₃-NPh)(CCPh)(CO)₁₀ (**2**) in low yield (Scheme 1). Complexes **1a** and **2** are stable in both the solution and solid states. The purification was carried out by thin-layer chromatography, followed by recrystallization from a mixture of CH₂Cl₂ and methanol at room temperature.

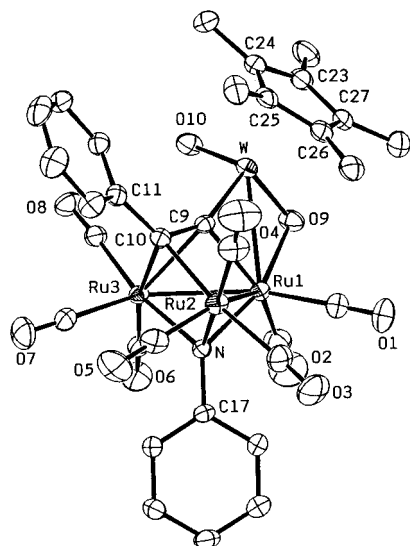
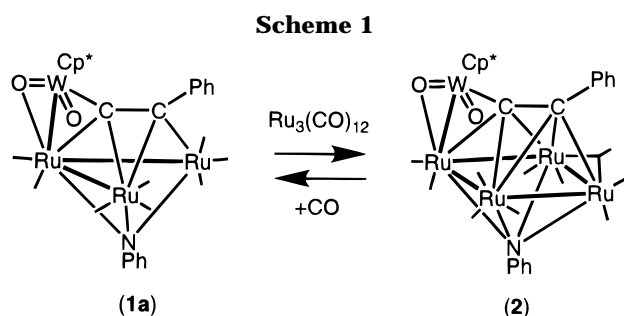


Figure 1. Molecular structure and atomic labeling scheme of the complex $(C_5Me_5)W(O)(\mu-O)Ru_3(\mu_3-NPh)(CCPh)(CO)_8$ (**1a**) with thermal ellipsoids shown at the 30% probability level.

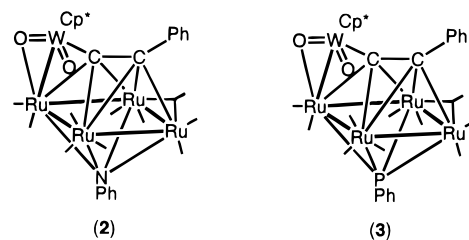


the acetylide ligand with respect to the Ru_3 plane are analogous to that observed in many group 8 trimetallic alkyne compounds exhibiting the so-called $2\sigma+\pi$ bonding mode.¹¹

Moreover, the tungsten atom is connected to the central $Ru(1)$ atom, C_α atom of the acetylide ligand, a terminal oxo ligand, and a bridging oxo ligand. The local arrangement of this tungsten atom resembles that of the mononuclear dioxo alkyl complexes $LW(O)_2(CH_2-SiMe_3)$, $L = Cp$ and C_5Me_5 , which possess a 16-electron configuration with two $W=O$ double bonds.¹² However, in complex **1a** the oxo atom O(10) adopts a terminal mode with distance $1.724(4)$ Å, resembling that of the terminal $W-O$ distances observed in the $W-Re$ complexes,¹³ while the second oxo ligand O(9) spans the $W-Ru(1)$ vector with $W-O(9) = 1.796(4)$ Å and $Ru(1)-O(9) = 2.182(4)$ Å, showing the $W=O$ double-bond character and formation of a dative interaction with the ruthenium atom. The key feature of the $W=O \rightarrow Os$

fragment in the related WO_3 cluster compounds which bear only one bridging oxo ligand¹⁴ and is also confirmed by the modest lengthening ($0.072(4)$ Å) of the $W=O$ distance for the bridging oxo ligand versus the terminal O(10) atom.

The second, minor product isolated from this reaction is the pentametallic cluster **2**. Although, no single-crystal X-ray analysis was carried out, its molecular structure was unambiguously identified by FAB mass analysis and by comparing its solution $\nu(CO)$ spectrum with that of the analogous phosphinidene cluster compound $(C_5Me_5)W(O)(\mu-O)Ru_4(\mu_3-PPh)(CCPh)(CO)_{10}$ (**3**).⁸ In agreement with this proposal, treatment of **1a** with $Ru_3(CO)_{12}$ in refluxing toluene gave the isolation of the expected cluster **2** in 47% yield. On the other hand, heating a solution of **2** under CO atmosphere led to the regeneration of **1a** in 86% yield. These reactions not only confirm the proposed structural assignment but also indicate that the pentametallic complex **2** is formed by a reversible cluster-building reaction, involving the insertion and removal of a $Ru(CO)_2$ fragment to the tetrametallic WRu_3 frame.



Condensation of $Ru_3(\mu_3-NPh)(CO)_{10}$ with $(C_5Me_5)W(O)_2(CCCMe=CH_2)$. To further extend the scope of this condensation reaction, the vinylacetylide complex $(C_5Me_5)W(O)_2(CCCMe=CH_2)$ was selected as an alternative precursor. Thus, treatment of $Ru_3(\mu_3-NPh)(CO)_{10}$ with $(C_5Me_5)W(O)_2(CCCMe=CH_2)$ in toluene afforded two tetrametallic clusters: $(C_5Me_5)W(O)(\mu-O)Ru_3(\mu_3-NPh)(CCCMe=CH_2)(CO)_8$ (**1b**) and $(C_5Me_5)W(\mu-O)_2Ru_3(\mu_3-NPh)(CCCMe=CH_2)(CO)_6$ (**4**) (Scheme 2). Again, these two complexes were separated by thin-layer chromatography and characterized by routine spectroscopic methods. The identification of **1b** is straightforward, as it displays an IR $\nu(CO)$ pattern similar to that of complex **1a**. In addition, in the 1H NMR spectrum in $CDCl_3$ solution, two signals at δ 5.65 and 5.39 with an intensity ratio of 1:1 are assigned to the olefinic protons of the vinyl substituent. As the observed chemical shifts resemble those observed for its precursor $(C_5Me_5)W(O)_2(CCCMe=CH_2)$,⁶ these spectral data confirm that the $C-C$ double bond of the vinylacetylide ligand is not coordinated to the ruthenium center.

On the other hand, the FAB mass analysis of **4** confirms the formula $C_{27}H_{25}O_8NRu_3W$ by showing the molecular ion at m/z 981 and the peaks due to the successful loss of six CO ligands. Consistent with this molecular formula, five $Ru-CO$ signals at δ 198.0,

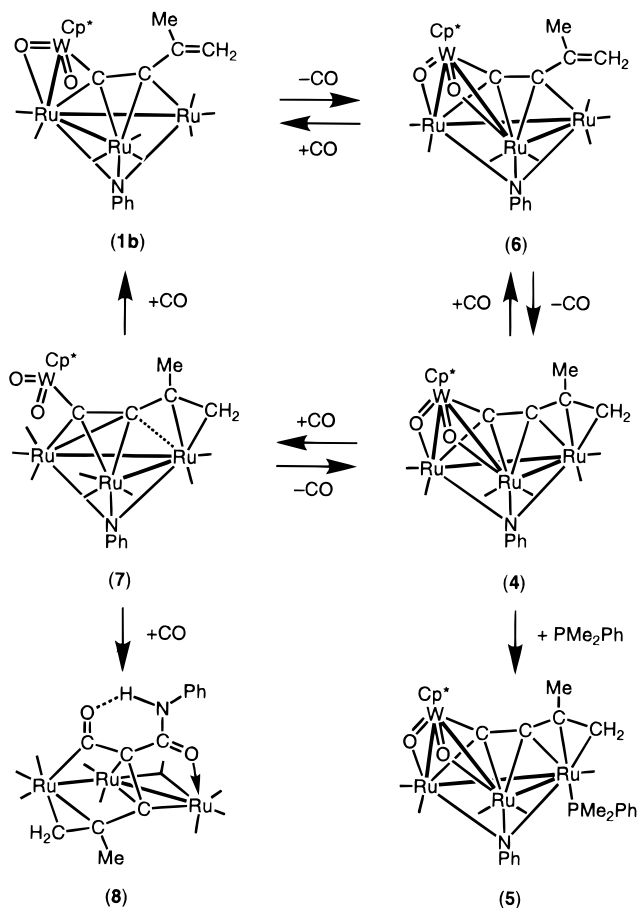
(11) Sappa, E.; Tiripicchio, A.; Braunstein, P. *Chem. Rev.* **1983**, *83*, 203.

(12) (a) Legzdins, P.; Rettig, S. J.; Sánchez, L. *Organometallics* **1985**, *4*, 1470. (b) Faller, J. W.; Ma, Y. *Organometallics* **1988**, *7*, 559. (c) Legzdins, P.; Veltheer, J. E. *Acc. Chem. Res.* **1993**, *26*, 41.

(13) (a) Chi, Y.; Cheng, P.-S.; Wu, H.-L.; Hwang, D.-K.; Peng, S.-M.; Lee, G.-H. *J. Chem. Soc., Chem Commun.* **1994**, 1839. (b) Wu, H.-L.; Lu, G.-L.; Chi, Y.; Farrugia, L. J.; Peng, S.-M.; Lee, G.-H. *Inorg. Chem.* **1996**, *35*, 6015. (c) Chi, Y.; Wu, H.-L.; Chen, C.-C.; Su, C.-J.; Peng, S.-M.; Lee, G.-H. *Organometallics* **1997**, *16*, 2443. (d) Chi, Y.; Wu, H.-L.; Peng, S.-M.; Lee, G.-H. *J. Chem. Soc., Dalton Trans.* **1997**, 1931.

(14) (a) Shapley, J. R.; Park, J.-T.; Churchill, M. R.; Ziller, J. W.; Beanan, L. R. *J. Am. Chem. Soc.* **1984**, *106*, 1144. (b) Chi, Y.; Shapley, J. R.; Ziller, J. W.; Churchill, M. R. *Organometallics* **1987**, *6*, 301. (c) Park, J. T.; Chi, Y.; Shapley, J. R.; Churchill, M. R.; Ziller, J. W. *Organometallics* **1994**, *13*, 813.

Scheme 2



197.9, 197.7, 196.1, and 194.7 were observed with a relative ratio 1:1:2:1:1 in the ^{13}C NMR spectrum. In addition to the CO signals, the signals at δ 160.2 ($J_{\text{WC}} = 37$ Hz) and 139.5 ($J_{\text{WC}} = 186$ Hz) are attributed to the acetylide C_β and C_α resonances, for which the assignments are made according to the magnitude of their J_{WC} coupling. Interestingly, the respective olefinic CMe and CH_2 signals of the vinyl fragment occur at δ 84.0 and 49.9, which are moved to the relative high-field position. Evidently, this change is due to the formation of vinyl to ruthenium metal coordination, a phenomenon that has been documented for the olefin cluster complexes.¹⁵ Similarly, the olefinic proton resonances of **4** appear at δ 4.09 and 3.55 in the ^1H NMR spectrum, showing a distinctive high-field shifting of 1.56 and 1.84 ppm with respect to **1b**.

Phosphine Substitution on 4. Complex **4** showed poor crystallinity and gave only the polycrystalline powdery materials during recrystallization in all attempts. As a result, no X-ray structural analysis was carried out to confirm the bonding of the vinylacetylide ligand. We then turned to study the reaction of **4** with PMe_2Ph with the hope to circumvent the difficulty in growing the suitable single crystals.

The phosphine complex $(\text{C}_5\text{Me}_5)\text{W}(\mu\text{-O})_2\text{Ru}_3(\text{CCCMe}=\text{CH}_2)(\mu_3\text{-NPh})(\text{CO})_5(\text{PMe}_2\text{Ph})$ (**5**) was obtained in moderate yield by heating a toluene solution containing **4** and 1 equiv of phosphine PMe_2Ph . The key spectral

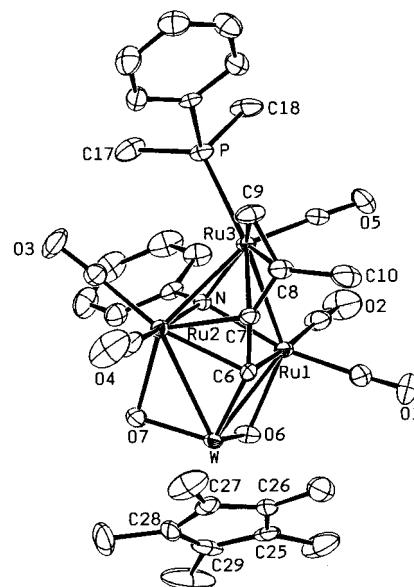


Figure 2. Molecular structure and atomic labeling scheme of the complex $(\text{C}_5\text{Me}_5)\text{W}(\mu\text{-O})_2\text{Ru}_3(\text{CCCMe}=\text{CH}_2)(\mu_3\text{-NPh})(\text{CO})_5(\text{PMe}_2\text{Ph})$ (**5**) with thermal ellipsoids shown at the 30% probability level.

data of **5** are the ^{13}C NMR data, which exhibit four signals at δ 159.5 ($J_{\text{WC}} = 37$ Hz, $J_{\text{PC}} = 10$ Hz), 140.7 ($J_{\text{WC}} = 184$ Hz, $J_{\text{PC}} = 3$ Hz), 80.6, and 49.2, attributed to the C_β and C_α resonances of the acetylide ligand and the CMe and CH_2 signals of the vinyl fragment, respectively. The successful assignment of these ^{13}C NMR signals indicated that its basic molecular geometry is analogous to that of **4**. Thus the X-ray analysis was carried out to reveal both the structure of **5** and its precursor **4**.

As indicated in Figure 2, the structure of **5** consists of a puckerd rhomboidal WRu_3 skeleton with two long W-Ru distances, $\text{W-Ru}(1) = 2.8057(6)$ Å and $\text{W-Ru}(2) = 2.8378(6)$ Å, and two short Ru-Ru distances, $\text{Ru}(1)\text{-Ru}(3) = 2.7618(7)$ Å and $\text{Ru}(2)\text{-Ru}(3) = 2.7543(7)$ Å, while the $\text{Ru}(1)\cdots\text{Ru}(2)$ distance ($3.2927(7)$ Å) is clearly out of the range expected for a significant Ru-Ru interaction. The $\text{Ru}(1)$ and $\text{Ru}(2)$ atoms each associates with two CO ligands, whereas the $\text{Ru}(3)$ atom is coordinated by one CO and a phosphine ligand. The oxo ligands span the W-Ru edges, showing the features expected for the double bridging $\text{W=O}\rightarrow\text{Ru}$ interaction, related to that of the dioxo complex $\text{CpWOs}_3(\mu\text{-O})_2(\mu\text{-H})(\text{CO})_9$.¹⁶ In addition, the vinylacetylide ligand adopts a novel $\mu_4\text{-}\eta^4$ -bonding mode, on which the C_α atom is linked to the W, $\text{Ru}(1)$, and $\text{Ru}(2)$ atoms, the C_β atom is associated with the $\text{Ru}(2)$ atom, and the vinyl fragment, $\text{C}(8)\text{-C}(9)$ vector, is coordinated to the $\text{Ru}(3)$ atom via π -donor interaction. The phenylimido ligand resides on the opposite side of the WRu_3 rhomboid. Interestingly, the $\text{Ru}(2)\text{-N}$ distance ($2.135(4)$ Å) is substantially longer than the other Ru-N distances, $\text{Ru}(1)\text{-N} = 2.099(4)$ and $\text{Ru}(3)\text{-N} = 2.058(4)$ Å. We speculate that the lengthening of the $\text{Ru}(2)\text{-N}$ distance is caused by the existence of the $\text{Ru}(2)\text{-C}(7)$ linkage. The extra electron density transferred to the $\text{Ru}(2)$ atom via this Ru-C bonding makes the $\text{Ru}(2)$ atom relatively more

(15) (a) Johnson, B. F. G.; Lewis, J.; Pippard, D. *J. Organomet. Chem.* **1981**, 213, 249. (b) Evans, J.; McNulty, S. C. *J. Chem. Soc., Dalton Trans.* **1984**, 79.

(16) Chi, Y.; Hwang, L.-S.; Lee, G.-H.; Peng, S.-M. *J. Chem. Soc., Chem. Commun.* **1988**, 1456.

electron rich, therefore weakening the corresponding Ru–N bonding.

Reaction of 4 with CO. The behavior of **4** with CO was extensively investigated. When this reaction was carried out in refluxing toluene solution, the regeneration of **1b** was obtained in nearly quantitative yield. Interestingly, if the complex **4** was exposed to CO atmosphere at room temperature for only 30 min, two new cluster complexes, $(C_5Me_5)W(\mu-O)_2Ru_3(\mu_3-NPh)(CCMe=CH_2)(CO)_7$ (**6**) and $(C_5Me_5)W(O)_2Ru_3(\mu_3-NPh)(CCMe=CH_2)(CO)_8$ (**7**), were isolated in moderate yields, together with the formation of **1b** in small amount.

For complex **6**, the ^{13}C NMR spectrum exhibits three Ru–CO signals at δ 197.0, 196.4, and 194.7 with an intensity ratio of 2:2:3 at room temperature. Apparently, the last CO signal at δ 194.7 is due to a $Ru(CO)_3$ fragment which undergoes rapid tripodal CO rotation, while the first two CO ligands at δ 197.0 and 196.4 are caused by two symmetrical $Ru(CO)_2$ units, each possessing two rigid and chemically distinct CO ligands. The acetylide C_α and C_β carbon signals are found to occur at δ 159.4 ($J_{WC} = 174$ Hz) and 182.7 ($J_{WC} = 33$ Hz), while the C_{Me} and CH_2 signals of the vinyl fragment appear at δ 150.1 and 117.6, respectively. Likewise, the 1H NMR signals attributable to the geminal vinyl proton resonances are clearly discernible at δ 5.42 and 5.23, indicating that the vinyl substituent is no longer attached to the Ru metal atom. Hence, the formation of **6** can be viewed as a CO coordination to the ruthenium atom, which then induced the departure of the vinyl π -interaction. This proposed structure is fully consistent with the X-ray analysis of an analogous cyclohexenyl derivative complex $(C_5Me_5)W(\mu-O)_2Ru_3(\mu_3-NPh)(CCC_6H_9)(CO)_7$.¹⁷

On the other hand, the FAB mass analysis of **7** indicates the possession of eight CO ligands, which are two CO ligands in excess to that of **4**. However, the vinyl group is strongly coordinated to the Ru atom, as the corresponding 1H and ^{13}C NMR signals all occurred at the high-field positions. This structural feature is unequivocally confirmed by the single-crystal X-ray crystallography. As can be seen from Figure 3, the Ru_3 framework of **7** forms an open triangular arrangement with distances $Ru(1)\cdots Ru(2) = 3.249(1)$ Å, $Ru(1)-Ru(3) = 2.7161(9)$ Å, and $Ru(2)-Ru(3) = 2.782(1)$ Å. The vinylacetylide ligand resides on the opposite side using both the acetylide and the vinyl π -interactions and is attached to a pendent $(C_5Me_5)W(O)_2$ fragment. It is clearly seen that two CO ligands have added to the terminal Ru(1) and Ru(2) metal atoms to compensate the unsaturation generated by the removal of $W=O \rightarrow Ru$ dative interactions. The $W=O$ distances and the $O=W=O$ bond angle are characteristic of those observed in the monometallic tungsten dioxo complexes.¹⁸

Reaction of 7 with CO. Complex **7** slowly converts to a light orange compound $Ru_3(CO)_9[C_6H_5O(CONHPh)]$ (**8**) upon exposure to CO atmosphere (40 psi). The first

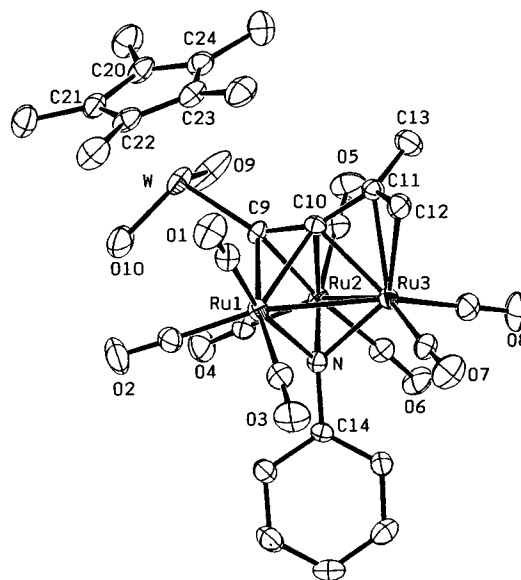


Figure 3. Molecular structure and atomic labeling scheme of the complex $(C_5Me_5)W(O)_2Ru_3(\mu_3-NPh)(CCMe=CH_2)(CO)_8$ (**7**) with thermal ellipsoids shown at the 30% probability level.

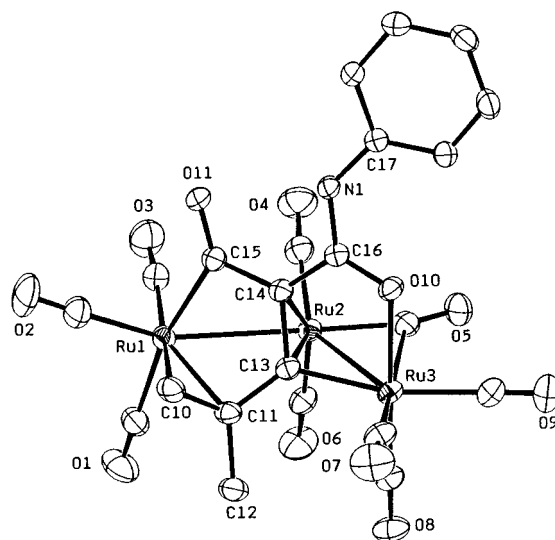


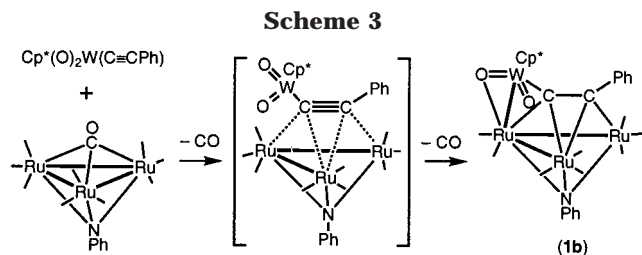
Figure 4. Molecular structure and atomic labeling scheme of the complex $Ru_3(CO)_9[C_6H_5O(CONHPh)]$ (**8**) with thermal ellipsoids shown at the 30% probability level.

indication of the removal of the $(C_5Me_5)W(O)_2$ fragment is provided by the 1H NMR spectrum which exhibited the absence of methyl signal of the (C_5Me_5) group. In fact, the FAB mass showed a parent molecular ion at $m/z = 771$, confirming the removal of the $(C_5Me_5)W(O)_2$ fragment, together with the incorporation of two CO ligands. The complex **8** was then subjected to a single-crystal X-ray diffraction study to reveal its identity.

As indicated in Figure 4, the structure of **8** consists of an open triangular arrangement of ruthenium atoms with distances $Ru(1)-Ru(2) = 2.8054(5)$ Å and $Ru(2)-Ru(3) = 2.8164(5)$ Å and obtuse bond angle $\angle Ru(1)-Ru(2)-Ru(3) = 114.67(2)^\circ$. The C(10) and C(11) atoms that constitute the vinyl group are coordinated to the Ru(1) atom, while the acetylide C_α and C_β carbon atoms C(13) and C(14) are mainly coordinated to the central Ru(2) atom. Interestingly, the C(14) atom of the acetyl-

(17) Selected crystal data: $C_{31}H_{29}NO_9Ru_3W$, orthorhombic, space group $P2_12_12_1$, $a = 12.835(2)$ Å, $b = 14.883(2)$ Å, $c = 17.371(5)$ Å, $Z = 4$, $\rho_{calcd} = 2.087$ g cm^{-3} , $F(000) = 1963$, $\mu = 48.96$ cm^{-1} , $R_r = 0.026$ and $R_w = 0.026$ for 3649 reflections with $I \geq 2\sigma(I)$.

(18) (a) Eagle, A. A.; George, G. N.; Tiekink, E. R. T.; Young, C. G. *Inorg. Chem.* **1997**, *36*, 472. (b) Harrison, W. M.; Saadeh, C.; Colbran, S. B.; Craig, D. C. *J. Chem. Soc., Dalton Trans.* **1997**, 3785.

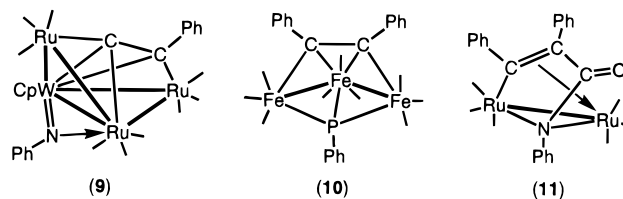


ide ligand is further linked to two CO fragments; one uses its oxygen atom O(10), forming a dative interaction to the Ru(3) atom, while the second CO ligand is coordinated to the Ru(1) atom through a direct Ru–C bonding. The phenylimido ligand is found to associate with the C(16) atom of the first CO fragment. The C(16)–N(1) distance (1.334(4) Å) is similar to the C–N single bond (~1.34 Å) observed in structures containing the bridging carboxamido functionality.¹⁹ Thus, it is best to consider that the imido N(1) atom is associated with an additional proton atom. In fact, the ¹H NMR spectrum of **8** showed the presence of a broad downfield resonance signal at δ 10.23, which is characteristic of the –NHPh proton experiencing an intramolecular hydrogen bonding with the oxygen atom of the carbonyl fragment, C(15)–O(11).

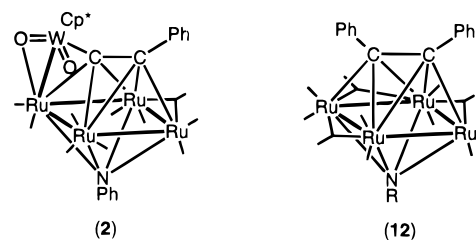
Discussion. The ruthenium cluster compounds **1a** and **1b** bearing a high-valent $(C_5Me_5)W(O)_2$ fragment can be prepared by combination of ruthenium carbonyl complex $Ru_3(CO)_{10}(\mu_3-NPh)$ with the dioxo acetylide complexes $(C_5Me_5)W(O)_2(CCR)$, R = Ph and $CMe=CH_2$. It should be noted that, for reaction using the phenylacetylide complex $(C_5Me_5)W(O)_2(CCPH)$, we obtained the formation of **1a** as the major product. Apparently, this reaction is initiated by the capping of the acetylide ligand to the Ru_3 frame (Scheme 3). The ligated acetylide then brought the $(C_5Me_5)W(O)_2$ fragment into the close vicinity of one $Ru(CO)_3$ unit and provided the driving force to induce the elimination of a CO and coordination of a $W=O$ fragment to the Ru atom. This proposed pathway is supported by the isolation of a butterfly WRu_3 cluster (**9**) from the condensation of acetylide complex $CpW(CO)_3(CCPH)$ and $Ru_3(\mu_3-NPh)(CO)_{10}$ ²⁰ and by the formation of alkyne cluster **10**, which contains an open triangular metal skeleton, from the reaction of phosphinidene cluster $Fe_3(\mu_3-PPh)(CO)_{10}$ with alkyne under UV photolysis.²¹ In the formation of **9**, the facile dissociation of CO ligands on tungsten has induced the migration of the imido ligand from the triruthenium face to the W–Ru edge, as the tungsten atom tends to interact more strongly with the electronegative nitrogen atom. However, during the formation of complexes **1a** and **1b**, no such ligand migration was observed due to the existence of strong bonding interaction between tungsten and oxo ligands.

To the contrary, the ruthenium imido cluster $Ru_3(CO)_{10}(\mu_3-NPh)$ reacts with diphenylacetylene to give the

binuclear metallapyrrolinone complex (**11**) exclusively.²² The latter observation implies that the alkyne coordination is rapidly accompanied by cluster fragmentation and C–N bond formation. Thus, we must not underestimate the cooperative donating effect of the dioxo tungsten unit in stabilizing the triruthenium frame during the formation of **1**, although we are unable to compare their relative donor capacity on the basis of our current evidence.



In addition, the reaction of $(C_5Me_5)W(O)_2(CCPH)$ with the trimetallic complex $Ru_3(CO)_{10}(\mu_3-NPh)$ leads to the formation of WRu_3 cluster compound **1**, while the analogous condensation reaction with the tetrametallic complex $Ru_4(CO)_{13}(\mu_3-PPh)$ affords the WRu_4 phosphinidene cluster **3**,⁸ which is isostructural to that of the imido cluster **2**, a thermodynamic product generated by the addition of a $Ru(CO)_2$ unit to **1**. Therefore, the conversion from **1** to **2** is best considered as a simple cluster-building reaction (Scheme 1). If we envision that the $(C_5Me_5)W(O)_2$ fragment acts as a two-electron donor similar to the CO ligand, complex **2** can be considered to possess a near rectangular $Ru_4(CO)_{11}$ frame with a symmetrical μ_4-NPh ligand and with a $\mu_4-\eta^2$ -metal-substituted alkyne ligand located on the other side. Such an arrangement of metal atoms, an imido ligand, and an alkyne is exactly identical to that observed in the homometallic imido compounds $Ru_4(\mu_4-NR)(PhCCPh)(CO)_{11}$ (**12**), R = H and Ph.²³



On the other hand, for the reaction of $Ru_3(CO)_{10}(\mu_3-NPh)$ with vinylacetylide complex $(C_5Me_5)W(O)_2(CCMe=CH_2)$, we obtained the formation of the related derivative complex **1b**. In contrast to the phenylacetylide derivative **1a**, where the phenyl group showed poor coordination capability, the vinyl substituent on **1b** can react with the adjacent ruthenium atom to form the η^4 -vinylacetylide ligand as observed in **4** (Scheme 2). Furthermore, as the terminal oxo group on the tungsten atom serves as a reasonably good electron donor, formation of an additional $W=O \rightarrow Ru$ interaction to replace one CO ligand also takes place. Interestingly, the Ru_3 framework also undergoes a skeletal rearrangement process which places the elongated, nonbonding Ru–

(19) (a) Lu, K.-L.; Chen, J.-L.; Lin, Y.-C.; Peng, S.-M. *Inorg. Chem.* **1988**, *27*, 1726. (b) Krone-Schmidt, W.; Sieber, W. J.; Boag, N. M.; Knobler, C. B.; Kaesz, H. D. *J. Organomet. Chem.* **1990**, *394*, 433. (c) Lin, P.-J.; Chi, Y.; Wang, S.-L.; Peng, S.-M.; Lee, G.-H. *J. Cluster Sci.* **1991**, *2*, 1.

(20) Chi, Y.; Hwang, D.-K.; Chen, S.-F.; Liu, L.-K. *J. Chem. Soc., Chem. Commun.* **1989**, 1540.

(21) (a) Knoll, K.; Orama, O.; Huttner, G. *Angew. Chem., Int. Ed. Engl.* **1984**, *23*, 976. (b) Knoll, K.; Huttner, G.; Zsolnai, L.; Orama, O. *Angew. Chem., Int. Ed. Engl.* **1986**, *25*, 1119.

(22) Han, S.-H.; Geoffroy, G. L.; Rheingold, A. L. *Organometallics* **1987**, *6*, 2380.

(23) (a) Song, J.-S.; Han, S.-H.; Nguyen, S. T.; Geoffroy, G. L. *Organometallics* **1990**, *9*, 2386. (b) Blohm, M. L.; Gladfelter, W. L. *Organometallics* **1986**, *5*, 1049.

Ru vector underneath the $(C_5Me_5)W(O)_2$ unit. A comparison of the structure of complexes **1a**, **5**, and **7** indicates that the variation of Ru–Ru bonds is collaborated by the coordination of the vinyl group to the Ru atom and the formation of two $W=O \rightarrow Ru$ interactions. Thus, the existence of the rigid and relatively large bond angle $\angle O=W=O \approx 106^\circ$ is responsible for the observed ruthenium skeletal isomerization. Of course, complex **4** is electron precise if we considered that the respective $W=O$ units, the vinylacetylide and the phenylimido ligand, each donates two, six, and four electrons to the $Ru_3(CO)_6$ framework, giving a total of 50 cluster valence electrons.

The cluster **4** was found to react quite differently with simple two-electron donors, such as phosphine or CO. The main product for the phosphine reaction was the monosubstituted complex **5**, in which the incoming phosphine attacked at the Ru atom that supported the vinyl substituent. For the reactions with CO, we isolated two addition products **6** and **7**, produced by the removal of the vinyl group from the Ru metal atom or the dissociation of $W=O \rightarrow Ru$ dative bonding, respectively. The formation of **6** and **7** is fully reversible; thus, heating a toluene solution of **6** or **7** under nitrogen leads to the regeneration of the parent complex **4** in high yields (Scheme 2).

Finally, although both complexes **6** and **7** were initially obtained from the treatment of **4** with CO, these complexes were fairly reactive under CO atmosphere upon raising the temperature, increasing the CO partial pressure, or extending the reaction time. Thus, treatment of **6** with CO in refluxing toluene solution gives rise to the formation of **1b**, confirming that complex **6** is the intermediate during the interconversion between **1b** and **4**. Remarkably, the reaction of **7** with CO at 30 °C gave a moderate yield of unexpected triruthenium cluster **8**, along with a trace amount of **1b** and other minor products that have not been identified. The X-ray structural study indicates that complex **8** is produced by linking two CO molecules to the C_α carbon of the vinylacetylide ligand, on which one CO then coupled with the imido ligand to afford the multisite-coordinated carboxamido CONHPh group. The observation of the carboxamido group and the effective elimination of the $(C_5Me_5)W(O)_2$ fragment probably suggest the participation of water as one reactant, which is undoubtedly present in trace amounts in the reaction system. It was our expectation that, after the addition of a proton to the imido ligand, the remaining hydroxyl group of water would react with the $(C_5Me_5)W(O)_2$ fragment to afford a hypothetical mononuclear complex $(C_5Me_5)W(O)_2(OH)$. Although we are unable to identify the presence of this mononuclear tungsten complex in the reaction mixture, the previous isolation of the anionic salt $[(C_5Me_5)W(O)_3]^-$ and the complex $(C_5Me_5)W(O)_2(OC_5Me_5)$ provides simple precedents,^{24,25} thus furnishing the necessary support of our proposed reaction.

Summary. The cluster compounds containing low-valent ruthenium atoms and a high-valent dioxo tung-

sten fragment $(C_5Me_5)W(O)_2$ were synthesized. These cluster compounds showed novel reactivity patterns involving the reversible cluster expansion and the intramolecular vinyl and oxo coordination, the latter attributable to the fact that both the vinyl and the oxo fragment are excellent donors to stabilize the unsaturation generated on the ruthenium atoms. In one case, cleavage of the pendent high-valent $(C_5Me_5)W(O)_2$ fragment was noted, along with the formation of a C–C bond between the acetylide and two CO ligands, and the protonation of the imido group.

Moreover, the reactions described herein provide a further model for the coexistence of an oxo early-metal unit and the low-valent, late-metal carbonyl fragment in one single molecule. Our observation complements the finding in the $RePt_3$ system in which up to three bridging oxo ligands were introduced by the direct reactions of $[Pt_3\{Re(CO)_3\}(\mu-dppm)_3]^+$ with various oxidants.²⁶ It should be noted that, unlike the binuclear complex $(C_5Me_5)W(O)_2-W(CO)_3(C_5Me_5)$,²⁷ where the tungsten atoms at two disparate oxidation states are held together by an unsupported metal–metal bonding, the formation of a W–Ru bond in complexes **1–6** is always associated with one bridging oxo ligand. This difference in reactivity is clearly caused by the retention of both $W=O$ multiple bonds and W–C(acetylide) bonding. Although the cleavage of the W–C bond has been successfully achieved during the formation of **8**, the dioxo tungsten fragment was found to dissociate from the triruthenium cluster frame. Perhaps the high oxophilicity of the tungsten atom is the major factor to support the oxo fragments and to prevent the completed transfer of the ligated oxo atom to the low-valent ruthenium atom, despite the fact that the ruthenium oxo carbonyl complexes have been prepared and isolated in several instances.²⁸

Acknowledgment. We thank the National Science Council of the Republic of China for financial support (Grant No. NSC 87-2113-M007-027-COM).

Supporting Information Available: Tables of atomic coordinates and anisotropic thermal parameters for complexes **1a**, **5**, **7**, and **8** (18 pages). Ordering information is given on any current masthead page.

OM980297Y

(24) Rau, M. S.; Kretz, C. M.; Geoffroy, G. L. *Organometallics* **1993**, *12*, 3447.

(25) Parkin, G.; Marsh, R. E.; Schaefer, W. P.; Bercaw, J. E. *Inorg. Chem.* **1988**, *27*, 3262.

(26) (a) Xiao, J.; Vittal, J. J.; Puddephatt, R. J.; Manojlovic-Muir, L.; Muir, K. W. *J. Am. Chem. Soc.* **1993**, *115*, 7882. (b) Xiao, J.; Hao, L.; Puddephatt, R. J.; Manojlovic-Muir, L.; Muir, K. W. *J. Am. Chem. Soc.* **1995**, *117*, 6316.

(27) Alt, H. G.; Hayen, H. I.; Rodgers, R. D. *J. Chem. Soc., Chem. Commun.* **1987**, 1795.

(28) (a) Colombié, A.; Bonnet, J.-J.; Fompeyrine, P.; Lavigne, G.; Sunshine, S. *Organometallics* **1986**, *5*, 1154. (b) Schauer, C. K.; Voss, E. J.; Sabat, M.; Shriver, D. F. *J. Am. Chem. Soc.* **1989**, *111*, 7662. (c) Mirza, H. A.; Vittal, J. J.; Puddephatt, R. J. *Inorg. Chem.* **1995**, *34*, 4239.